Structure–Reactivity Effects in the Breakdown of Hemiacetals of α-Bromoacetophenone. Change in Rate-Limiting Step for Base Catalysis

Poul E. Sørensen,*,† K. J. Pedersen,† P. R. Pedersen,† V. M. Kanagasabapathy,‡ and Robert A. McClelland*,‡

Contribution from the Chemistry Department A, The Technical University of Denmark, DK-2800, Lyngby, Denmark, and Department of Chemistry, University of Toronto, Toronto, Ontario, Canada M5S 1A1. *Received August 3, 1987. Revised Manuscript Received March 8, 1988*

Abstract: Kinetics of breakdown are reported for the ethyl, methyl, 2-chloroethyl, and 2,2,2-trifluoroethyl hemiacetals of α-bromoacetophenone, the hemiacetals being generated by the aqueous bromination of the appropriate α-alkoxystyrene. Acid catalysis is characterized by a Brønsted α value of 0.6 and a β_{lg} (for H^+) of 0.3. With these values the transition state has been located on a reaction coordinate diagram for the class e mechanism of acid catalysis and a comparison made with positions of transition states for acetaldehyde and formaldehyde hemiacetals. With changing electrophilicity of the carbonyl there is a consistent shift in the position of the transition state, but the effect is relatively small. The base-catalyzed breakdowns of the ethyl and 2-chloroethyl hemiacetals have β values near 0.7, significantly higher than the values associated with analogous formaldehyde and acetaldehyde hemiacetals. The difference can be explained in terms of the reaction coordinate diagram of the class n base mechanism, recognizing the decreased susceptibility of the ketone to nucleophilic addition. With the trifluoroethyl hemiacetal, buffer dilution plots are curved and there is a downward break in the rate–pH profile. These are explained by a mechanism—hemiacetal ⇄ hemiacetal anion → product—where at low buffer concentrations or low H^+ concentration the deprotonation step is rate-limiting. As shown through a kinetic analysis, rate-limiting proton transfer is a result of a large rate constant for anion breakdown (≈8×10^8 s^{-1}). Thus, at low buffer concentration breakdown occurs more quickly than reprotonation. The curvature arises because the buffer acid provides efficient protonation. At high buffer concentration the deprotonation step is (approaching) a rapid equilibrium preceding rate-limiting breakdown. Comparison with the other two hemiacetals shows that the behavior of the trifluoroethyl compound is predictable on the basis of structure–reactivity correlations. A reaction with rate-limiting proton transfer is enforced by the very short lifetime of the hemiacetal anion.

The general-acid–base-catalyzed breakdown of aldehyde hydrates and hemiacetals[1,2] has been shown in recent studies to involve a class n base reaction (eq 1) and a class e acid reaction (eq 2). These mechanisms have been established for hemiacetals

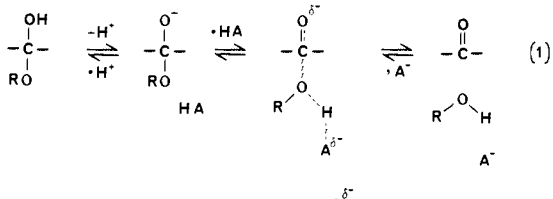

(1)

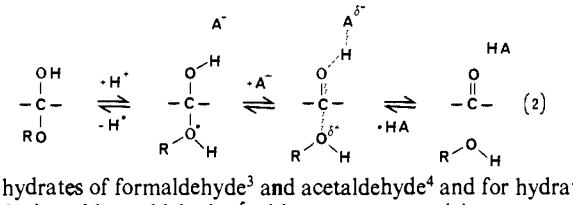

(2)

and hydrates of formaldehyde[3] and acetaldehyde[4] and for hydrates of substituted benzaldehydes,[5] with structure–reactivity parameters being the principal criteria. Analysis of the formaldehyde data in terms of energy contour diagrams provides additional support for the class n mechanism,[6] but suggests that the acid reaction also involves proton transfer between the alcohol leaving group and solvent in the transition state.[7]

We have been interested in the effect of substituent changes that decrease the lifetime of the hemiacetal anion intermediate of the base reaction. Our previous investigations have involved cyclic systems with phenol[8] and carboxylate[9] leaving groups, where the class n mechanism appears no longer to be followed. In this paper we report a study of four hemiacetals of α-bromoacetophenone. This represents an extension to the ketone level, where the carbonyl has become very stable. Unlike formaldehyde and acetaldehyde, the aldehydes studied extensively previously,[3,4]

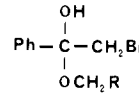

R = CH_3, H, CH_2Cl, CF_3

α-bromoacetophenone shows no sign of hydration in water. Indeed, this structural change results in an interesting mechanistic variation in the base reaction of the trifluoroethyl hemiacetal, enforced by a very short lifetime of the hemiacetal anion.

Experimental Section

Materials. α-Methoxystyrene was prepared by the cracking of acetophenone dimethyl ketal.[10] Other α-alkoxystyrenes were prepared by the reaction of ethyl benzoate, 2-chloroethyl benzoate, and 2,2,2-trifluoroethyl benzoate with Tebbe's reagent, with purification by chromatography.[11]

α-Methoxystyrene: ^1H NMR ($CDCl_3$) δ 3.76 (3 H, s), 4.23 (1 H, d, J = 3 Hz), 4.68 (1 H, d, J = 3 Hz), 7.25–7.75 (5 H, m).

† The Technical University of Denmark.
‡ University of Toronto.

(1) Bell, R. P. *Adv. Phys. Org. Chem.* **1966**, *4*, 1–29.
(2) Jencks, W. P. *Acc. Chem. Res.* **1976**, *9*, 425–432.
(3) Funderburk, L. H.; Aldwin, W. P.; Jencks, W. P. *J. Am. Chem. Soc.* **1978**, *100*, 5444–5459.
(4) Sørensen, P. E.; Jencks, W. P. *J. Am. Chem. Soc.* **1987**, *109*, 4675–4690.
(5) McClelland, R. A.; Coe, M. *J. Am. Chem. Soc.* **1983**, *105*, 2718–2725.
(6) Grunwald, E. *J. Am. Chem. Soc.* **1985**, *107*, 4710–4715.
(7) Grunwald, E. *J. Am. Chem. Soc.* **1985**, *107*, 4715–4720.
(8) McClelland, R. A.; Devine, D. B.; Sørensen, P. E. *J. Am. Chem. Soc.* **1985**, *107*, 5459–5463.
(9) McClelland, R. A.; Sørensen, P. E. *Can. J. Chem.* **1986**, *64*, 1196–1200.
(10) Loudon, G. M.; Smith, C. K.; Zimmerman, S. E. *J. Am. Chem. Soc.* **1974**, *96*, 465–479.
(11) Tebbe, F. N.; Parshall, G. W.; Reddy, G. S. *J. Am. Chem. Soc.* **1978**, *100*, 3611–3613. Pine, S. H.; Zahler, R.; Evans, D. A.; Grubbs, R. H. *Ibid.* **1980**, *102*, 3270–3272. Pine, S. H.; Pettit, R. J.; Geib, G. D.; Cruz, S. G.; Gallego, C. H.; Tijerina, T.; Pine, R. D. *J. Org. Chem.* **1985**, *50*, 1212–1216.

0002-7863/88/1510-5118$01.50/0

Table I. Catalytic Coefficients for the Breakdown of Bromoacetophenone Hemiacetals [M^{-1} s^{-1}, 25 °C ionic strength = 1.0 ($NaClO_4$)]

catalyst	pK_{HA}	OCH_2CH_3	OCH_3	OCH_2CH_2Cl
H_3O^+ [a]	−1.74[b]	154 ± 9	120 ± 3	47 ± 3
$CHCl_2COOH$	1.26[c]	9.0 ± 8	8.2 ± 1.0	2.5 ± 0.1
$CH_2ClCOOH$	2.70[b]	0.75 ± 0.08	0.67 ± 0.01	0.30 ± 0.02
$Cl(CH_2)_2COOH$	3.93[b]	0.25 ± 0.01	0.17 ± 0.01	0.025 ± 0.003
CH_3COOH	4.65[b]	0.06 ± 0.02	0.06 ± 0.01	
H_2O [f]	−1.74[b]	0.005 ± 0.004	0.007 ± 0.005	0.015 ± 0.004
$ClCH_2CO_2^-$	2.70[b]	[e]	[e]	[e]
$Cl(CH_2)_2CO_2^-$	3.3[b]	0.03 ± 0.01	0.28 ± 0.01	0.34 ± 0.02
$CH_3CO_2^-$	4.65[b]	0.27 ± 0.01	0.69 ± 0.02	0.62 ± 0.06
$(CH_3)_3CCO_2^-$	4.80[b]	0.34 ± 0.04	[d]	1.8 ± 0.3
$(CH_3)_2AsO_2^-$	6.16[b]	4.8 ± 0.08	14.6 ± 0.5	13 ± 1
HPO_4^{2-}	6.49[h]	7.7 ± 2	25 ± 3	22 ± 10
OH^- [i]	15.74[b]	(1.6 ± 0.2) × 10^7	(5.4 ± 0.3) × 10^7	(6.5 ± 0.5) × 10^8

[a] Rate constants based upon experiments in 0.01–0.50 M $HClO_4$ and molar concentration of H_3O^+. [b] Reference 4. [c] Sander, E. G.; Jencks, W. P. *J. Am. Chem. Soc.* **1968**, *90*, 4377–4386. [d] Not determined. [e] Not detectable. [f] *units* of s^{-1}. [g] See text for origin of these numbers. [h] Fox, J. P.; Jencks, W. P. *J. Am. Chem. Soc.* **1974**, *96*, 1436–1449. [i] Based upon activities calculated as $10^{pH-13.7}$.

α-Ethoxystyrene: ^1H NMR ($CDCl_3$) δ 1.42 (3 H, t, J = 7 Hz), 3.94 (2 H, q, J = 7 Hz), 4.17 (1 H, d, J = 3 Hz), 4.62 (1 H, d, J = 3 Hz), 7.25–7.75 (5 H, m).

α-2-Chloroethoxystyrene: ^1H NMR ($CDCl_3$) δ 3.75 (2 H, distorted t, J = 6 Hz), δ 4.03 (2 H, distorted t, J = 6 Hz), 4.13 (1 H, d, J = 3 Hz), 4.60 (1 H, d, J = 3 Hz), 7.15–7.65 (5 H, m).

α-2,2,2-Trifluoroethoxystyrene: ^1H NMR ($CDCl_3$) δ 4.25 (2 H, q, J = 8 Hz), 4.25 (1 H, d, J = 3 Hz), 4.85 (1 H, d, J = 3 Hz), 7.27–7.74 (5 H, m); MS for $C_{10}H_9F_3O$, m/z calcd 202.0606, found 202.0600.

Kinetics. A 10^{-4} M solution of α-alkoxystyrene in 0.01 M NaOH was mixed with an equal volume of a solution containing (2–5) × 10^{-4} M bromine, 0.01 M $HClO_4$, and the appropriate buffer. The ionic strength was maintained at 1 M with $NaClO_4$ in both solutions, and the temperature was 25 °C. Most of the kinetic runs were carried out on a Durrum Gibson stopped-flow spectrophotometer, although a few were sufficiently slow that conventional spectroscopy could be employed. Increases in absorbance due to the formation of α-bromoacetophenone were followed at 250 nm. Rate constants, k_{obsd}, were calculated as the slopes of plots of ln (A_∞ − A) versus time or with use of the Swinbourne–Kezdy procedure. Excellent first-order behavior was observed in all cases.

Results and Discussion

Hemiacetal Generation. The method employed to study hemiacetals of α-bromoacetophenones has been described previously.[12] The three-stage aqueous bromination of α-alkoxystyrenes has a bromination stage approaching the diffusion limit,[13] and this is followed by a very rapid cation hydration[14,15] (eq 3). Thus, with

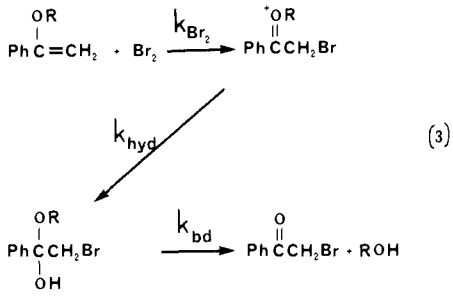

(3)

bromine in excess over alkoxystyrene, and at a concentration greater than 100 μM, the first two stages are complete within microseconds. The product at this point is the hemiacetal, and its conversion to products can be monitored by following the appearance of the α-bromoacetophenone at 250 nm.

Hemiacetal Breakdown Kinetics. This bromination procedure serves as a general approach, working even with the 2,2,2-trifluoroethoxy system where the electron-withdrawing group might have slowed the initial bromination. Rate constants were obtained at ionic strength 1.0 in $HClO_4$ solutions, and in dichloroacetate, chloroacetate, 3-chloropropionate, acetate, cacodylate, and biphosphate buffers.[17] Catalysis by the added buffers was observed,

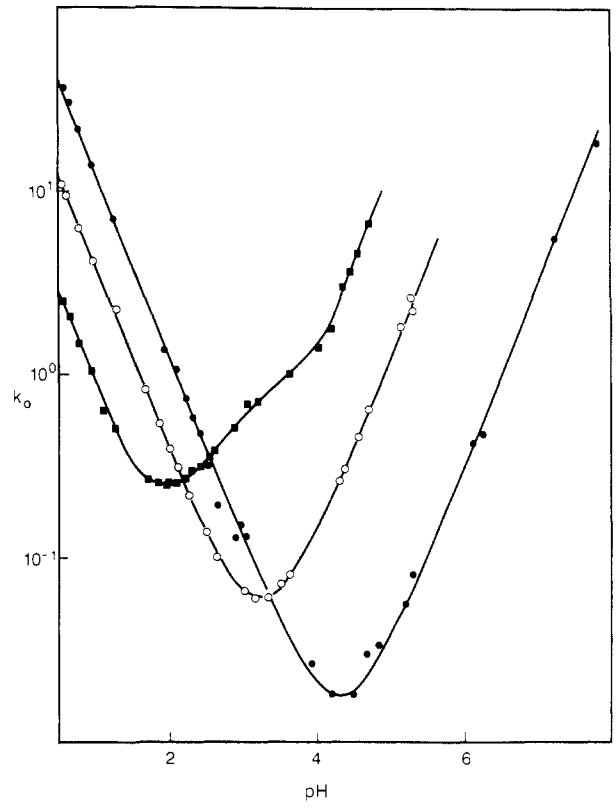

Figure 1. Rate–pH profiles for breakdown of α-bromoacetophenone hemiacetals: (●) ethyl, (○) 2-chloroethyl, (■) 2,2,2-trifluoroethyl. The points are experimental and are based upon rate constants in $HClO_4$ solutions (pH <3.1) or by extrapolation to zero buffer concentration. The lines for ethyl and 2-chloroethyl have been drawn according to the formula $k_H[H^+] + k_o + k_{OH}[OH^-]$, using parameters given in Table I. For a discussion of the more complex curve for trifluoroethyl, see the text.

Table II. Brønsted α and β Values for Acid-Catalyzed and Base-Catalyzed Breakdown of α-Bromoacetophenone Hemiacetals

hemiacetal	α	β
ethyl	0.6	0.71
methyl	0.62	0.72
2-chloroethyl	0.75	0.66

(12) Kanagasabapathy, V. M.; McClelland, R. A. *J. Chem. Soc., Chem. Commun.* **1985**, 691–692.
(13) Ruasse, M. F.; Angile, A.; Dubois, J. E. *J. Am. Chem. Soc.* **1984**, *106*, 4846–4849.
(14) Young, P. R.; Jencks, W. P. *J. Am. Chem. Soc.* **1977**, *99*, 8238–8248.
(15) McClelland, R. A.; Ahmad, M. *J. Am. Chem. Soc.* **1978**, *100*, 7031–7036.
(16) A plot of log k_{H^+} versus pK_{ROH} for the α-bromoacetophenone hemiacetals, including k_{H^+} = 9.7 M^{-1} s^{-1} for trifluoroethyl, is excellently linear with a slope of 0.33.
(17) There is one drawback in that bromine reacts with several of the buffers commonly employed in studying hemiacetal breakdown.

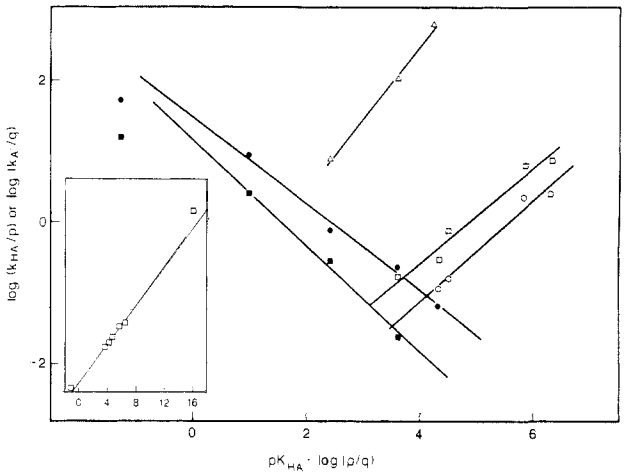

Figure 2. Brønsted plots for general-acid and general-base catalysis of the breakdown of α-bromoacetophenone ethyl hemiacetal (●, ○) and 2-chloroethyl hemiacetal (■, □) and 2,2,2-trifluoroethyl hemiacetal (k_3 rate constant, Δ). The inset incorporates the water and hydroxide points with the base data for the 2-chloroethyl hemiacetal. The line is the linear regression line for the points in the main figure.

and with the exception of the trifluoroethyl hemiacetal, plots of k_{obsd} versus buffer concentration were linear. The data were treated in the normal fashion[3-5] to give catalytic coefficients for the acid and base components of the buffer (Table I). Again, with the exception of the trifluoroethoxy compound, rate–pH profiles took the expected form (Figure 1). From these, rate constants were calculated for H^+, OH^-, and water (Table I) with the precision of the values for the latter very low because of the sensitivity to the other catalysts particularly OH^-. The water rates for the ethoxy and methoxy hemiacetals may not be statistically significant.

Brønsted plots for the ethyl and 2-chloroethyl hemiacetals are shown in Figure 2. These are perhaps less well-defined than those obtained in the formaldehyde and acetaldehyde studies, partly because of the limited number of buffers that could be employed,[17] and additionally because the steepness in the plots further limited the range over which each type of catalysis is exhibited. Bronsted α and β values are given in Table II, the α values being calculated without the H_3O^+ point, which has a slight negative deviation. Although small variations in α and β with substituent might be expected,[3-5] the values for each type of catalysis in Table II are probably not statistically different because of the limited data available. In consequence we will not attempt to analyze the substituent variations, as has been done previously.[3-5] The inset shows an extended base catalysis plot for the chloroethyl hemiacetal. The hydroxide ion rate shows a slight positive deviation, while the water rate lies quite close to the line. The latter situation is observed with other hemiacetals[3-5] and is normally taken as evidence that water is acting as a simple base catalyst.

Figure 3 depicts a reaction coordinate diagram for the rate-limiting step of the acid reaction (eq 2). This diagram has been drawn as previously described,[3-5] and with the experimental α and β_{lg} values, the transition state has been located for three ethyl hemiacetals for the reaction with H^+ catalysis. In explaining the difference between CH_2O and CH_3CHO, it was argued[4] that the CH_3 group in the latter results in a stabilization of the protonated aldehyde (P_+) and, to a lesser extent, a stabilization of the neutral aldehyde (P_o). These changes result in a movement of the transition state perpendicular to the reaction coordinate toward P_+ (an anti-Hammond effect) and a movement parallel to the reaction coordinate toward R_+ (Hammond effect). Similar reasoning predicts that the trend should continue with α-bromoacetophenone. The change $CH_3CHO \rightarrow PhCOCH_2Br$ destabilizes R_+ relative to P_o since in the bromo ketone systems the tetrahedral forms are less stable. Moreover, the CH_2Br and Ph groups will further destabilize the protonated hemiacetal through an inductive effect. Both factors therefore predict a Hammond effect movement of the transition state for $PhCOCH_2Br$ toward

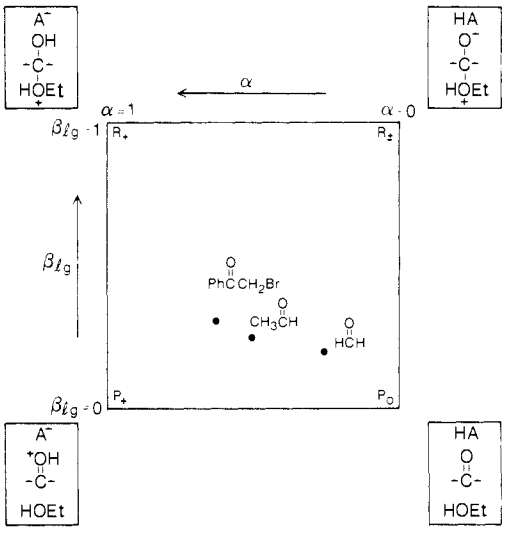

Figure 3. Reaction coordinate diagram for the rate-limiting step of the class e mechanism for acid-catalyzed ethyl hemiacetal breakdown. The *x* and *y* axes represent proton transfer and C–O bond breaking/formation as measured by α and β_{lg}, respectively. The positions of transition states have been indicated for the H_3O^+ reactions using α = 0.28, β_{lg} = 0.20 for formaldehyde ethyl hemiacetal,[3] α = 0.51, β_{lg} = 0.25 for acetaldehyde ethyl hemiacetal,[4] and α = 0.62, β_{lg} = 0.33[16] for α-bromoacetophenone ethyl hemiacetal.

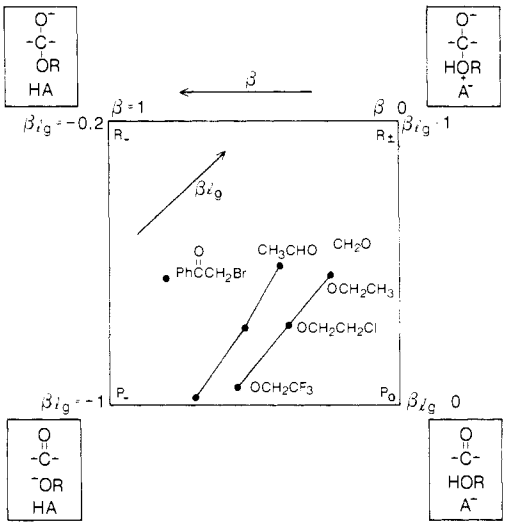

Figure 4. Reaction coordinate diagram for the rate-limiting step of the class n mechanism for base-catalyzed hemiacetal breakdown. The *x* and *y* axes represent proton transfer and C–O bond breaking/formation. The positions of the transition states have been indicated for the reactions catalyzed by acetate. The positions for formaldehyde and acetaldehyde are based upon β and β_{lg} values calculated by appropriate differentiation of eq 7 of ref 4, using the interaction parameters given there. The bromoacetophenone point has β = 0.7, β_{lg} = −0.4.

R_+. In addition, the P_+ corner should be stabilized relative to $R_\pm$ for $PhCOCH_2Br$, with a resulting anti-Hammond movement toward the former. The overall prediction is that the $PhCOCH_2Br$ transition state should be more to the left-hand side of the diagram, with a greater α value and probably greater β_{lg} than that found with CH_3CHO. This clearly is observed, although it is interesting considering the difference in susceptibility of the three carbonyls to nucleophilic addition that there is remarkably little movement in the transition-state position. This has been noted previously and also applies when different catalysts and different ROH are considered.[4]

The class n base reaction, in its breakdown direction, has a rate-limiting step with general-acid catalysis of C–O bond cleavage of the hemiacetal anion. In contrast to the acid reaction, the transition state moves considerably with structural variation. A reaction coordinate diagram for the rate-limiting step is provided

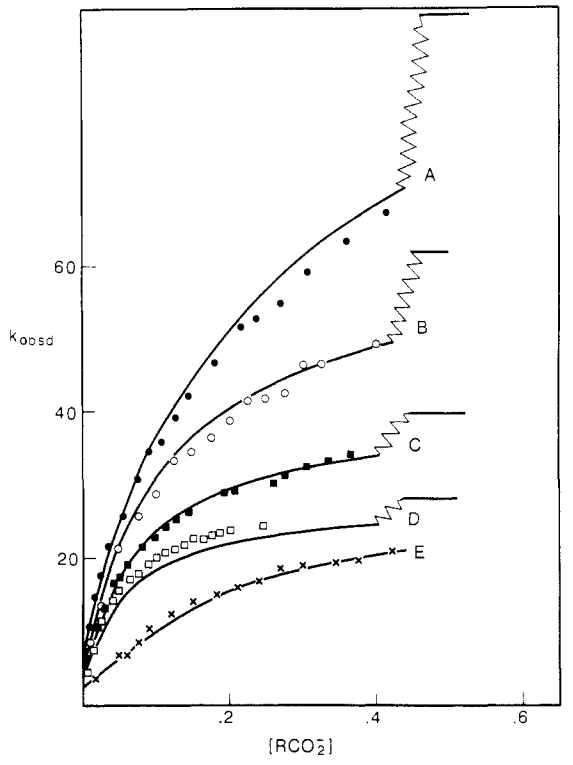

Figure 5. Buffer dilution plots of constant pH for the breakdown of α-bromoacetophenone trifluoroethyl hemiacetal. Sets A–D are acetate buffers: A, HA:A$^-$ = 4:6, pH = 4.70; B, HA:A$^-$ = 1:1, pH = 4.55; C, HA:A$^-$ = 6:4, pH = 4.35; D, HA:A$^-$ = 2:1, pH = 4.21. Set E is a 3-chloropropionate buffer: HA:A$^-$ = 1:3, pH = 4.32. The points are experimental. The lines are drawn according to eq 6, using constants discussed in the text.

in Figure 4, with the position of the transition state indicated for three hemiacetals each of formaldehyde and acetaldehyde and for catalysis by acetate ion. The diagonal movement from $R_\pm$ to P_-, which occurs with each aldehyde with an increase in electron withdrawal in ROH, is an anti-Hammond effect arising from a stabilization of the P_- corner relative to $R_\pm$. The movement toward the left-hand edge for the change $CH_2O \rightarrow CH_3CHO$ represents a combination of anti-Hammond and Hammond effects, which tend to make the transition state slide toward P_- and R_-, respectively. The explanation for this is that with the less electrophilic aldehyde CH_3CHO, the bottom edge of the diagram is lowered in energy relative to the top edge.

α-Bromoacetophenone is less electrophilic again, and therefore, this trend should continue. This does seem to be the case. The β values are now quite large, ~0.7, locating the transition state well to the left-hand side of the diagram. Our β_{lg} values are not so well-defined because of the limited set of data. We have used in Figure 4 a value of −0.4, calculated with the ethoxy and 2-chloroethoxy rate constants[18] and with the assumption of a linear plot of log k versus pK_{ROH}. Such plots are not linear for CH_2O and CH_3CHO,[3,4] and for this reason, the −0.4 value is best regarded as an average for the two alcohols in question. Whatever the exact position with respect to the β_{lg} axis, the transition state is clearly located in a position consistent with the CH_2O and CH_3CHO behavior. Thus, in the breakdown direction with $PhCOCH_2Br$ only a small amount of proton transfer from the catalyzing acid is required to reach the transition state.

Trifluoroethyl Hemiacetal. The unusual feature with this hemiacetal is the curvature of the buffer dilution plots (Figure 5), a behavior usually indicative of a change in rate-limiting step with changing buffer concentration.[19] Our analysis is based upon the accepted mechanisms for base catalysis, with the recognition that the proton transfer may be rate-limiting.

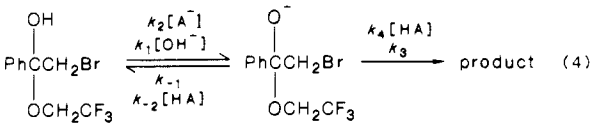

(4)

As an initial simplification, the HA-catalyzed breakdown, the k_4 process, will be ignored; the importance of this will be discussed later. A stationary state treatment in the anion produces the equation

$$k_{obsd} = \frac{\frac{k_1}{1 + k_{-1}/k_3}[OH^-] + \frac{k_2}{1 + k_{-1}/k_3}[A^-]}{1 + \frac{k_2(k_{-1}/k_3)}{k_1(1 + k_{-1}/k_3)}\frac{[A^-]}{[OH^-]}} \quad (5)$$

This derivation recognizes that the rate constants are not all independent, since

$$K_a = k_1 Kw/k_{-1} = k_2 K_{HA}/k_{-2} \quad (6)$$

where K_a and K_{HA} represent acidity constants for the hemiacetal and buffer acid, respectively.

Equation 5 takes the form

$$k_{obsd} = \frac{A[OH^-] + B[A^-]}{1 + C[A^-]/[OH^-]} \quad (7)$$

For the four sets of acetate buffers the variation in k_{obsd} with [A$^-$] was fit to eq 7 with nonlinear least squares to obtain the three parameters that best satisfy the data at each pH. These were then averaged to give $A = (7.2 \pm 1.0) \times 10^9$ M^{-1} s^{-1}, $B = (5.4 \pm 1.0) \times 10^2$ M^{-1} s^{-1}, and $C = (6.1 \pm 1.1) \times 10^{-9}$ M^{-1} s^{-1}. The curves drawn in Figure 5 show the overall fit using the above three values. The individual fits at each pH were better. The deviations occur on taking one value each for A–C, and probably arise from slight variations in pH, which was ±0.02 with each buffer ratio.

Equation 5 has been written in such a way that it contains three independent quantities, and these can be calculated[20] from A–C as $k_1 = (7.8 \pm 1.1) \times 10^9$ M^{-1} s^{-1}, $k_2 = (5.9 \pm 1.1) \times 10^2$ M^{-1} s^{-1}, and $k_{-1}/k_3 = 0.09 \pm 0.03$. Through eq 6 we also calculate $k_{-2}/k_3 = 9.1 \pm 1.3$ M^{-1} and $k_3K_a/K_w = (9 \pm 2) \times 10^{10}$ M^{-1} s^{-1}. One set of data each was also obtained with a chloropropionate buffer and a chloroacetate buffer. These data were fit to eq 5 by fixing the buffer independent k_1 and k_{-1}/k_3 at the values obtained from the acetate analysis, so that there was only one variable k_2. Values obtained were $(1.1 \pm 0.2) \times 10^2$ M^{-1} s^{-1} for $ClCH_2CH_2CO_2^-$ and 8 ± 1 M^{-1} s^{-1} for $CH_2ClCO_2^-$. The curve drawn through set E in Figure 5 is the result of this fit.

Two points of consistency can be noted. The rate constants k_2 refer to simple proton transfers proceeding in the thermodynamically unfavorable direction. A Brønsted plot based upon the three values has a slope of 0.96, within experimental error of the expected value of unity. The rate constant k_1 on the other hand represents a thermodynamically favorable proton transfer (see K_a estimate later), and this number is within the range expected for such a reaction.[21]

The values of k_{-1}/k_3 and k_{-2}/k_3 provide an explanation behind the buffer curvature. The former being less than unity signifies that the hemiacetal anion, when formed in the absence of buffer, proceeds on to product rather than reprotonate. Thus, formation of anion, a proton transfer, is rate-limiting. In terms of eq 5, k_{obsd} at zero buffer is equal to $k_1[OH^-]/(1 + k_{-1}/k_3)$, which is approximately $k_1[OH^-]$—a rate-limiting deprotonation by OH$^-$. Addition of buffer initially accelerates, and the dependency ap-

(18) The data for the methylhemiacetal has been ignored. With CH_2O and CH_3CHO the points for this alcohol show positive deviations in plots of log k versus pK_{ROH}, and that would appear to be the case here as well.[3,4]

(19) Jencks, W. P. *Catalysis in Chemistry and Enzymology*; McGraw-Hill: New York, 1968; p 465.

(20) $(k_{-1}/k_3) = AC/(B - AC)$; $k_1 = AB/(B - AC)$; $k_2 = B^2/(B - AC)$; $k_{-2}/k_3 = BCK_{HA}/K_w(B - AC)$; $k_3K_a/K_w = B/C$; $K_w = 10^{-13.7}$: Harned, H. S.; Owen, B. B. *The Physical Chemistry of Electrolytic Solutions*, 3rd ed., Reinhold: New York, 1958.

(21) Eigen, M. *Angew. Chem., Int. Ed. Engl.* **1964**, *3*, 1–72.

Table III. Rate Constants and Equilibrium Constants for the Breakdown of α-Bromoacetophenone Hemiacetals

	CH_3CH_2	$ClCH_2CH_2$	CF_3CH_2	acetaldehyde CF_3CH_2
pK_a	12.39	12.05	11.66	13.14[a]
k_{-1}, s^{-1}	4×10^{8} [b]	1.8×10^{8} [b]	7×10^{7}	2×10^{9}
k_{-2}, $M^{-1}\ s^{-1}$	7×10^{9} [c]	7×10^{9} [c]	7×10^{9}	7×10^{9} [c]
k_3, s^{-1}	8×10^{5} [d]	1.4×10^{7} [d]	8×10^{8}	7×10^{7} [d]
k_4, $M^{-1}\ s^{-1}$ [e]	7×10^{6} [f]	2×10^{7} [f]	$\approx 10^{8}$	1.3×10^{8} [f]
k_{-1}/k_3	5×10^{2}	13	0.087	15

[a] Reference 2. [b] $k_{-1} = k_1K_w/K_a$ with $k_1 = 8 \times 10^9\ M^{-1}\ s^{-1}$, $pK_w = 13.7$ [c] Assumed to be the same as the CF_3CH_2 value. [d] $k_{OH}K_w/K_a$, with k_{OH} = catalytic coefficient for hydroxide ion catalysis. [e] For acetic acid as catalyst. [f] $k_{OAc}K_{HOAc}/K_a$ with $pK_{HOAc} = 4.6$ and k_{OAc} = catalytic coefficient for acetate anion catalysis.

proximates as $k_2[A^-]/(1 + k_{-1}/k_3)$, which simplies to $k_2[A^-]$—a rate-limiting deprotonation by the buffer base. Addition of buffer, however, also increases the rate of anion protonation via the k_{-2} process, and with k_{-2}/k_3 greater than unity, at high buffer concentrations $k_{-2}[HA]$ is greater than k_3. This signifies that the anion now returns to neutral hemiacetal faster than it goes on to products, a situation corresponding to rate-limiting breakdown. In the limit, k_{obsd} levels at a value of $k_3K_a[OH^-]/K_w$ and is no longer dependent upon buffer concentration (although it does depend upon pH). At this plateau the mechanism is the same as that associated with OH^- catalysis for less reactive hemiacetals. Taking the k_{OH} values for ethyl and 2-chloroethyl, and the plateau k_3K_a/K_w for trifluoroethyl, a good correlation is in fact seen with the alcohol leaving group ability. With the two former hemiacetals the k_{OH} values are based upon extrapolation to zero buffer, as is normally done. The zero buffer value for trifluoroethyl, however, does not fit on the correlation since it refers to a different rate-limiting step.

The kinetic analysis furnishes numerical values for k_1 and k_2 and ratios only of the other rate constants. Their individual values can be calculated through an estimate of the hemiacetal acidity constant. The Hine equation provides a pK_a value of 12.09 for the hydrate of α-bromoacetophenone.[22] Following Jencks, a statistical correction is made to arrive at a pK_a value for the ethyl hemiacetal, and then other values are obtained with the assumption that a $pK_a - pK_{ROH}$ correlation has a slope of 0.2.[3,4] Table III lists these pK_a values, along with individual rate constants. A further consistency can be noted in the trifluoroethyl analysis, in that the k_{-2} value lies within the expected range. This rate constant refers to protonation of the anion by buffer acid, a proton transfer in the thermodynamically favored direction.

The ethyl and chloroethyl hemiacetals clearly exhibit a catalysis by general bases. This reaction mechanistically arises from HA-catalyzed breakdown of the hemiacetal anion. This reaction, the k_4 process of eq 5, was neglected in the analysis of the trifluoroethyl data. An evaluation of its importance can be made by noting (Table III) that a correlation of k_4 with alcohol leaving group ability, using the two values for ethyl and chloroethyl, predicts a k_4 value of $\approx 10^8\ M^{-1}\ s^{-1}$ for trifluoroethyl. With this hemiacetal, however, k_3, the rate constant for noncatalyzed anion breakdown, is very large, $\sim 10^9\ s^{-1}$. The consequence is that even in 1 M HA the k_4 process can only contribute 10% to the overall rate, and this would be very difficult to detect. A contribution from the k_4 process would give rise to an additional term in the kinetic expression, such that at high buffer concentration k_{obsd} would not level but would continue to increase.[23] The buffer plots have in fact not leveled, but this is not inconsistent with the simple treatment, since HA concentrations of 5–10 M are necessary for k_{obsd} to be truly constant. With the experimental uncertainty, a small contribution from the k_4 process would be missed. Inclusion of this reaction in the kinetic analysis however does not improve the fit.

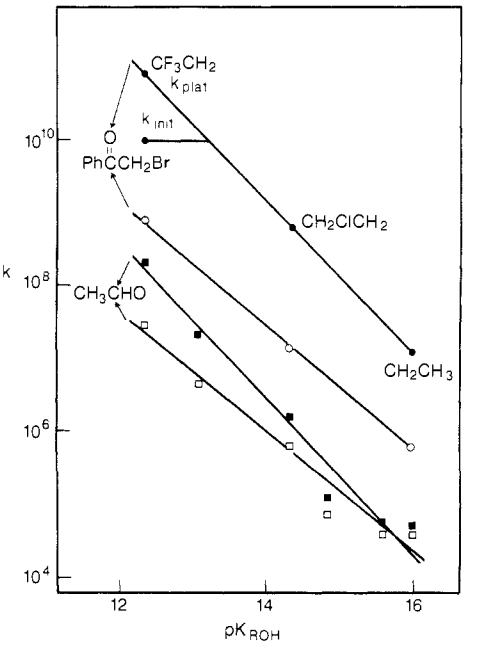

Figure 6. Leaving group dependences for k_{OH} (●, ■) and k_3 (○, □) for α-bromoacetophenone and acetaldehyde hemiacetals (data for the latter from ref 4). For the bromoketone trifluoroethyl hemiacetal, k_{init} is the hydroxide ion rate constant at zero buffer concentration $[k_1/(1 + k_{-1}/k_3)]$, while k_{plat} is the rate constant at infinite buffer concentration (k_3K_a/K_w). Slopes of the lines are −1.05, −0.85, −1.07, and −0.87 proceeding down the diagram.

The trifluoroethyl hemiacetal also exhibits an unusual rate–pH profile, with a downward break near pH 3 (Figure 1).[24] This behavior can be accounted for by a mechanism again with a change in rate-limiting step, this time with changing pH (eq 8).

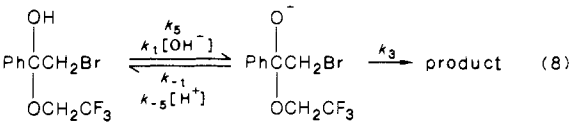

A quantitative treatment, which would be similar to that of ref 24b, will not be attempted here, since the break is not particularly pronounced, and moreover, a different reaction, that involving the class e H^+ catalysis, takes over below pH 2. In quantitative terms, $k_{-1} \approx 10^8\ s^{-1}$ (Table III) and $k_{-5} \approx 10^{11}\ M^{-1}\ s^{-1}$.[21] Thus, at $[H^+] < 10^{-4}$, $k_{-1} > k_{-5}[H^+]$, and the protonation of the hemiacetal anion occurs with the solvent (the k_{-1} process).[25] With $k_{-1} < k_3$, deprotonation is rate-limiting. As $[H^+]$ is increased, however, anion protonation by H^+ becomes more important and a stage is reached where $k_{-1} + k_{-5}[H^+]$ becomes greater than k_3. This corresponds to a situation where anion protonation is faster than breakdown, and the latter is therefore rate-limiting.

In summary, rate-limiting proton transfer with the trifluoroethyl hemiacetal is enforced by the short lifetime of the anionic intermediate. The reverse reaction, the addition of trifluoroethoxide anion to α-bromoacetophenone, has a trapping mechanism[26] where the addition step is an equilibrium and there is rate-limiting proton transfer to the anionic adduct. At low buffer concentrations buffer acid can accelerate the overall addition by providing an additional route for this proton transfer. Table III illustrates how the k_{-1}/k_3 ratio changes with changing alkoxy group. The rate constant k_3

(22) (a) For $R_1R_2C(OH)_2$, $pK_a = 14.19 - 1.315\ [\sigma^*(R_1) + \sigma^*(R_2)]$[22b]; $\sigma^*(Ph) = 0.60$, $\sigma^*(CH_2Br) = 1.00$. (b) Hine, J.; Koser, G. F. *J. Org. Chem.* **1971**, *36*, 1348–1351.

(23) For an example with a hydrogen ortho ester where a change in rate-limiting step of the same type occurs, but the rate constants do not level at high buffer concentration, see: McClelland, R. A. *J. Am. Chem. Soc.* **1984**, *106*, 7579–7583.

(24) (a) Breaks in rate–pH profiles of the same type observed here have recently been reported for the ring opening of 2-hydroxy-1,3-dithiolanes.[24b] (b) Okuyama, T. *J. Am. Chem. Soc.* **1984**, *106*, 7134–7139. Okuyama, T.; Fueno, T. *Ibid.* **1985**, *107*, 4224–4229.

(25) This is the justification for ignoring the k_{-5} process in the analysis of the buffer data.

(26) Jencks, W. P. *Acc. Chem. Res.* **1980**, *13*, 161–169.

increases dramatically with increased electron withdrawal (Figure 6; $\beta_{lg} = -0.95$[27]), while k_{-1} decreases slightly ($\beta = 0.2$[28]). The ethyl and chloroethyl hemiacetals have $k_{-1}/k_3 > 1$, and proton transfer therefore cannot be rate-limiting. A crossover is predicted when the leaving alcohol has a pK_{ROH} of ~ 13. The data for the acetaldehyde trifluoroethyl system illustrate the importance of the k_{-1} rate constant as well. With this hemiacetal k_3 has become large, but since the anion is a stronger base by ~ 1.5 pK_a units than the anion derived from the bromoketone, k_{-1} is also large, and k_{-1}/k_3 is still greater than unity.

(27) Because of the way pK_a is calculated, this β_{lg} is simply the value experimentally determined for OH^- catalysis minus 0.2.
(28) This arises because of the assumption of a 1/5 relationship between ΔpK_a and ΔpK_{ROH}.

Acknowledgment. The financial support of the Natural Sciences and Engineering Research Council of Canada is gratefully acknowledged. We also thank Statens Naturvidenskabelige Forskningsraad for an equipment grant.

Kinetics of Amphiphilic Ketone Epimerizations in Cleavable Surfactant Hosts

David A. Jaeger,*,‡ Phillip K. Chou,‡ Durgadas Bolikal,‡ Dong Ok,† Kwang Yoo Kim,† Jeffrey B. Huff,† Eun Yi,† and Ned A. Porter*,†

Contribution from the Department of Chemistry, Duke University, Durham, North Carolina 27706, and the Department of Chemistry, University of Wyoming, Laramie, Wyoming 82071. *Received November 30, 1987*

Abstract: The rate of epimerization and product equilibrium composition of eight amphiphilic ketone diastereomers were determined in aqueous base and in surfactants that were stable to strong base but were cleaved to nonsurfactant compounds upon mild acid workup. These cleavable surfactant hosts gave equilibria for the amphiphilic ketones similar to cetyltrimethylammonium bromide and dicetyldimethylammonium bromide, which were models for these structures. Furthermore, rates of ketone equilibration determined in these cleavable surfactant hosts indicate an appreciable catalytic effect for equilibration, as compared to equilibrations of the amphiphilic ketones in aqueous base alone. One of the ketone surfactant pairs was studied above and below its critical micelle concentration (cmc). Below the cmc, rates of equilibration were high and no diastereoselectivity was observed in the equilibration while above the cmc of the substrate, rates of equilibration were lower and the meso diastereomer was favored.

Molecular aggregates, such as micelles and lipid bilayer membranes, are important structures in biology and chemistry,[1-3] and they have functions such as emulsion polymerization catalysts,[4] structural components in complex biological systems,[5] and hosts for membrane-bound enzyme catalysts.[6] It has been established that these aggregates have important catalytic properties and their influence on rates of reactions has been reported on numerous occasions.[2,4,7-10] The effect of micelles and lipid bilayers on the stereochemical course of organic reactions has also been reported, and recent publications indicate a dramatic influence of aggregates on the rates of reactions of chiral reactants.[11-13]

We have recently reported that the hydrophobic effect can be used to perturb equilibria of two-chain ketone surfactants, such as **1-3**.[14,15] These epimerizable ketones exist as meso and (±) diastereomers, and the equilibrium ratio (base or acid catalyzed) of these diastereomers is 50:50 in isotropic fluids but is perturbed to as much as 90:10 in favor of the meso diastereomer if the base-catalyzed equilibrations are carried out in aqueous molecular aggregates. Equilibrations of **1-3** were also carried out in the presence of excess authentic micelle-forming cationic surfactant cetyltrimethylammonium bromide (CTAB) and with the bilayer-forming cationic surfactant dicetyldimethylammonium bromide (DDAB).[16-18] These surfactant hosts perturb the equilibrium ratios obtained from the twin-chain surfactants, as compared to equilibrations carried out without added cationic surfactants. While CTAB increases the meso/(±) product ratio for the 6,6′-linked ketone **2**, the equilibrium ratio for the 9,9′-linked ketone **3** decreases in CTAB relative to the value obtained in water alone. On the other hand, the bilayer-forming surfactant DDAB increases the equilibrium product ratio for both ketones **2** and **3**.

In the course of these studies with CTAB and DDAB, it became apparent that ketone equilibria were established faster in the presence of these cationic surfactants than was the case without these positively charged hosts.[15] Thus, equilibrium for **3** at 60 °C without CTAB or DDAB required over 200 h. On the other hand, the equilibrium for **3** could be established in a matter of a few hours at 60 °C with CTAB or DDAB present, and equilibrations could be achieved at 37 °C in a matter of days with these

† Duke University.
‡ University of Wyoming.

(1) Fendler, J. H. *Chem. Br.* **1984**, *20*, 1098.
(2) Fendler, J. H. *Membrane Mimetic Chemistry*; Wiley: New York, 1982.
(3) Menger, F. M. *Nature (London)* **1985**, *313*, 603.
(4) Fendler, J. H.; Fendler, E. J. *Catalysis in Micellar and Macromolecular Systems*; Academic: New York, 1975.
(5) Schwyzer, R. *Biochemistry* **1986**, *25*, 4281.
(6) Mimms, L. T.; Zampighi, G.; Nozaki, Y.; Tanford, C.; Reynolds, J. A. *Biochemistry* **1981**, *20*, 833.
(7) Bunton, C. A. *Catal. Rev.-Sci. Eng.* **1979**, *20*, 1.
(8) Romsted, L. S. In *Micellization, Solubilization, and Microemulsions*; Mittal, K. L., Ed.; Plenum: New York, 1977; Vol. 2, p 509.
(9) Quina, F. H.; Chaimovich, H. *J. Phys. Chem.* **1979**, *83*, 360.
(10) Cipiciani, A.; Germani, R.; Savelli, G.; Bunton, C. A. *J. Chem. Soc., Perkin Trans.* II **1985**, 527.
(11) Moss, R. A.; Chiang, Y.-C. P.; Hui, Y. *J. Am. Chem. Soc.* **1984**, *106*, 7506.
(12) Ueoka, R.; Moss, R. A.; Swarup, S.; Matsumoto, Y.; Strauss, G.; Murakami, Y. *J. Am. Chem. Soc.* **1985**, *107*, 2186.
(13) Moss, R. A.; Schreck, R. P. *Tetrahedron Lett.* **1985**, *26*, 6305.
(14) Porter, N. A.; Ok, D.; Adams, C. M.; Huff, J. B. *J. Am. Chem. Soc.* **1986**, *108*, 5025.
(15) Porter, N. A.; Ok, D.; Huff, J. B.; Adams, C. M.; McPhail, A. T.; Kim, K. *J. Am. Chem. Soc.* **1988**, *110*, 1896.
(16) Kunitake, T. *Ann. N. Y. Acad. Sci.* **1986**, *471*, 70.
(17) Kunitake, T.; Okahata, Y.; Anoda, S.; Hirakawa, S.-I. *J. Am. Chem. Soc.* **1980**, *102*, 7877.
(18) Shimomura, M.; Kunitake, T. *Chem. Lett.* **1981**, 1001.

0002-7863/88/1510-5123$01.50/0